Electrical Power and Energy Systems 162 (2024) 110308

Contents lists available at ScienceDirect

International Journal of Electrical Power and Energy Systems

journal homepage: www.elsevier.com/locate/ijepes

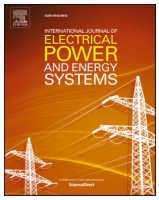

Damping control in renewable-integrated power systems: A comparative analysis of PSS, POD-P, and POD-Q strategies

Marta Bernal-Sancho [a,*], María Paz Comech [b], Noemí Galán-Hernández [a]

[a] Electrical Systems Department, CIRCE Technology Centre, Zaragoza 50018, Spain
[b] ENERGAIA Mixed Research Institute (CIRCE Technology Centre and University of Zaragoza), Zaragoza 50018, Spain

ARTICLE INFO

Keywords:
Low Frequency Oscillation
Inter-area Oscillation
Local Oscillation
Power System Stabilizer
Power Oscillation Damping
Renewable Energy

ABSTRACT

The shift from traditional fossil fuel-based power systems to renewable energy sources heightens the importance of frequency regulation. The lack of inertia in this new generation increases the risk of low-frequency oscillatory events, a significant concern in power systems stability. To mitigate these stability problems, it is crucial to study the effectiveness of damping controllers. This paper delves into the analysis of three damping controllers: the power system stabilizers (PSS) installed in synchronous generators, and two Power Oscillation Damping (POD) controllers, one with active power modulation (POD-P) and the other with reactive power modulation (POD-Q), typically installed in environments with high renewable penetration.

The main objective is to critically evaluate the comparative advantages of PSS, POD-P, and POD-Q controllers in local and inter-area oscillations by exploring their flexibility and performance under various initial conditions and oscillatory scenarios. The proper choice of damping controllers will ensure the stability of the grid in future scenarios of high renewable production, thus allowing the definition of future technology needs. This research is of utmost importance as it aims to dampen different oscillations by employing uniform control parameters in the PSS, POD-P, and POD-Q controllers. Five scenarios are defined on a system based on the IEEE 39 Bus New England System model and simulated by DIgSILENT PowerFactory. The results are analyzed methodically per scenario, facilitating a comparative evaluation of the controllers and reaching promising conclusions.

1. Introduction

The transition to renewable energy sources (RES) like wind turbines and photovoltaic (PV) plants is redefining power generation, driven by environmental and economic imperatives, apart from the global trend towards decarbonization and the imperative role of renewable energy in this context. This shift from traditional fossil fuel-based synchronous generators is unsafe from a power system point of view, as their inherent inertia has been vital for frequency regulation and overall system stability. Inertia acts as a damper against sudden load or generation changes, helping maintain stable frequency levels. When wind generation is integrated into the grid, it displaces synchronous generators, reducing the overall inertia of the system. This reduction in inertia affects frequency and voltage stability and increases susceptibility to low-frequency oscillatory (LFO) events [1]. Moreover, the intrinsic variability and lack of inertia in RES, especially wind and photovoltaic generation, pose challenges in maintaining frequency stability and system robustness [2,3], which must be flexible and reliable to support renewable energy supply [4]. These challenges are exacerbated during intense power transients, heightening the potential for LFO events, which are significant in power systems with high-RES penetration. LFO can be categorized into local oscillations (with a frequency from 0.7 to 2.0 Hz) occurring within a specific area and inter-area oscillations (with a frequency from 0.1 to 0.7 Hz) happening between groups of generators [5].

Traditionally, power system stabilizers (PSS) have managed LFOs, improving the stability by modulating the excitation of synchronous generators [6]. However, due to the transition to RES, there has been much research on integrating flexible AC transmission system (FACTS) devices with power oscillation damping (POD) controllers to enhance power control and system stabilization. Some authors [5–17] propose that while PSSs effectively damp local oscillations, their impact on inter-area oscillations is more limited. They argue that this limitation highlights the need for POD controllers, prompting coordinated studies to understand their effectiveness in overall system stabilization. The most common FACTS studied are the static synchronous compensator (STATCOM) [7,8], the thyristor-controlled series compensator (TCSC)

* Corresponding author.
E-mail address: mbernal@fcirce.es (M. Bernal-Sancho).

https://doi.org/10.1016/j.ijepes.2024.110308
Received 16 May 2024; Received in revised form 5 September 2024; Accepted 9 October 2024
Available online 16 October 2024

Nomenclature

RES	Renewable Energy Sources
PV	Photovoltaic
LFO	Low-Frequency Oscillatory
PSS	Power System Stabilizers
FACTS	Flexible AC Transmission System
STATCOM	Static Synchronous Compensator
TCSC	Thyristor Controller Series Compensator
UPFC	Unified Power Flow Controller
POD	Power Oscillation Damping
POD-P	Power Oscillation Damping, Active Power
POD-Q	Power Oscillation Damping, Reactive Power
DSPF	DIgSILENT PowerFactory
AVR	Automatic Voltage Regulator
PPC	Power Plant Controller
RMS	Root Mean Square

[9–13], or the unified power flow controller (UPFC) [14–16]. Furthermore, other comparative studies have been conducted to examine the damping capabilities of PSS in conjunction with FACTS-POD systems [17–19]. Moreover, some authors studied FACTS-POD using Wide-Area Damping Controllers (WADC) to enhance the damping of interarea oscillations [20,21].

In response to these developments, grid codes worldwide are starting to optionally require a power oscillation damping controller in RES and storage, focusing on increasing frequency and voltage stability. This leads to some issues in the controller, as the power park modules' voltage and reactive power control characteristics should not adversely affect the damping of power oscillations [22]. Some examples are the European Commission [23], Spain [24], Finland [25], and Australia [26], are evolving to mandate damping services from RES [27,28]. According to the grid codes, comparative studies have probed the damping capabilities of a PV plant with POD-P and POD-Q controllers under various conditions, considering different scenarios or factors such as communication channel delays [29–32]. Furthermore, in [33,34], the authors compare POD-P and POD-Q, focusing on damp oscillation individually and together, displaying the time domain results and considering the same initial conditions [33] or adapting the parameters when a change in the grid dynamics is detected [34].

As for wind power plants, some authors propose a POD controller to guarantee power system resiliency during power oscillations [35–38]. Other studies analyze the impact of integrating large amounts of wind power, exploring various control strategies to improve damping or delving into the wind turbines' oscillatory nature [39]. Some researchers focus on optimizing the parameters of Wind-POD and PSS controllers to ensure robustness against system uncertainties [40,41]. Another study delves into the details of wind turbines to evaluate the effects of POD controllers on turbine integrity, introducing a comprehensive model considering the electrical, structural, and aerodynamic characteristics [42].

Investigations have also targeted optimal node selection for POD and PSS in systems with significant wind penetration, examining the influence of variables such as transmission distance and tie-line power [43,44].

Previous research has often compared the damping efficacy of Wind-POD and PSS using static initial conditions, and only the LFOs associated with one scenario are considered without a broad array of scenarios. Nevertheless, if different scenarios are considered, they are limited by the small scale of the two-grid, four-machine IEEE system, and the controller settings are recalculated for each scenario. This approach does not reflect the reality of power systems, where controller settings are usually constant for all disturbances. Moreover, previous studies maintain that PSS is only suitable for damping local oscillations and has limitations for damping inter-area ones.

The main objective of the research presented in this paper is to evaluate the efficiency, flexibility, and performance of PSS, POD-P, and POD-Q. Leveraging the advanced simulation tools of DIgSILENT PowerFactory (DSPF) [45] and a network based on the IEEE 39 Bus New England System model [46], this study provides innovative insights into the adaptability and robustness of these control mechanisms. By analyzing system behavior in five initial scenarios, this research delineates the comparative advantages and potential limitations of each control strategy (PSS, POD-P, and POD-Q) in damping various low-frequency oscillations, emphasizing their role in maintaining grid stability in an energy landscape increasingly dominated by renewable sources with low inherent inertia. To consider different operating conditions due to the inherent uncertainty of renewable production, the loss of each one of the controllers is also evaluated as a critical scenario. This research aims to enrich the knowledge base on grid stability in the renewable energy era, providing new perspectives and solutions to the challenges ahead.

The article is organized as follows. Section 2 explains the composition of the PSS, POD-P, and POD-Q controller blocks and their operation. Section 3 describes the simulated network based on IEEE 39 Bus New England System model. Section 4 defines the five different scenarios under study, which are the starting point for analyzing the controller behavior to damp them. Section 5 discusses the results of damping the different oscillations by employing uniform control parameters in the PSS, POD-P, and POD-Q controllers. The results are analyzed methodically by scenario, emphasizing the importance of the comparative evaluation of the controllers. For this purpose, in the different simulations, the POD-P, POD-Q, or PSS controllers will be activated individually at each generation node. Section 5 also includes an N-1 contingency analysis for each oscillation scenario to elucidate the controller performance and uncover possible failure mechanisms, thus improving the operational reliability of damping controllers in practical environments. Furthermore, a summary and discussion of the main characteristics of the damping controllers are presented at the end of Section 5. Finally, Section 6 includes the conclusions obtained throughout the study.

2. Definition of the Damping Controllers

As highlighted in the introduction (Section 1), the research delves into the behavior of three controllers for damping low-frequency oscillations. This section provides a comprehensive understanding of these controllers, namely PSS, POD-P, and POD-Q, detailing the parameters that require adjustment. Understanding these controls is pivotal for this research and for the field of power system engineering as a whole.

2.1. Power System Stabilizer, PSS

The primary function of the PSS is to add damping to the generator rotor by controlling its excitation through an auxiliary stabilizer signal. To provide damping, the stabilizer must produce an electrical torque component in phase with the rotor speed deviations [5].

Fig. 1 depicts the block diagram of the PSS model used in the article. The PSS consists of three main blocks: a gain block, a signal washout block, and a two-stages phase compensation block (lead/lag block) [5].

Since the purpose of a PSS is to introduce a damping torque component, the speed of the synchronous machine on which the PSS is installed (xspeed) can be used as a local signal to control the generator's excitation. The PSS processes the information about the oscillations and provides a command to the exciter to dampen the electrical system's oscillations (upss). The output, *upss*, is an additional input to the automatic voltage regulator (AVR).

The gain K_{pss} determines the amount of damping introduced by the PSS. Ideally, the gain should be set at a value corresponding to maximum damping. The signal washout block serves as a high pass

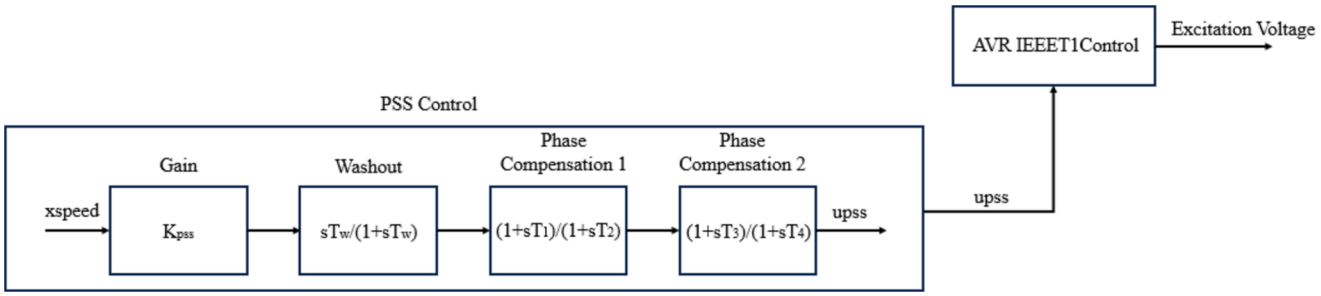

Fig. 1. PSS model block diagram

filter, with a time constant T_w high enough (in the range of 1 to 20 seconds) to pass stabilizing signals at the frequencies of interest unchanged but not so long that it leads to undesirable generator voltage excursions during system islanding conditions. Without it, steady changes in speed would modify the terminal voltage. It allows the PSS to respond only to changes in speed. The phase compensator block provides the appropriate phase-lead to compensate for the phase lag between the exciter input and the generator electrical torque. In this case, two blocks are used to achieve the desired block compensation [5]. All the parameters described above must be parameterized to damp the oscillation.

2.2. Power Oscillation Damping, POD

The POD's main objective is the same as that of the PSS [5]: to damp power oscillations. POD control is introduced in FACTS, wind, or PV plants to give them the same damping qualities as the synchronous generators. The POD controller attached to the renewable plant could be placed in the power plant controller (PPC), sending the same damping signal to all generators or into each generator individually. In this article, a POD controller installed into the PPC is considered.

Fig. 2 shows the block diagram of the POD-P model installed in the PPC active power control. The POD-P control is added as a supplementary control loop to the active power controller, adding an additional reference sent to the wind turbines, *dP_POD*. The POD-P diagram can be applied to POD-Q controllers. The only difference between them is that, in the case of the POD-Q, the control branch is added to the reactive control of the PPC, and the sign of the input signal is changed. In the case of the POD-P control, the sign is negative, so the active power injection is opposite the frequency deviation.

The POD controller consists of the same three main blocks as the PSS, the parameters to be set being a stabilizer gain K_{pod}, a washout filter with time constant T_w, and two-phase compensation blocks with time constants T_{b1}, T_{a1}, T_{b2}, and T_{a2}. The POD receives input containing oscillation information from the power system, such as the active power, voltage, or frequency. This article considers the frequency of the terminal where the wind farm is connected as input (*frequency*). The output of the POD control (*dP_POD*) provides the command for damping the oscillation as an extra reference added to the generator controller's original active or reactive power reference [40,29].

3. Network Description

This paper presents the development and analysis of five different scenarios to generate different LFOs in the system in the simulated network whose single-line diagram is illustrated in Fig. 3. This network is based on the New England IEEE-39 power system model, which is a simplified representation of the transmission system in the northeastern region of the United States, as described in [46]. The original IEEE-39 model comprises 39 buses, 10 generators, 19 loads, 34 lines, and 12 transformers. In this study, several wind farms in enough proportion to affect power oscillation damping have been connected. As shown in Fig. 3, five new wind power plants have been connected to the network, sharing the same terminal with traditional synchronous generators to preserve the initial generation nodes. Furthermore, to maintain the power flows in the network, the new wind farms will provide half of the power initially supplied by conventional generation at each node. The wind power plants, the synchronous generators, and the terminals where they are connected are highlighted in Fig. 3 by the black squares, indicating the name of the wind generators and the damping controllers from each generation node.

In this network, Generator *G01* represents the interconnection with the rest of the transmission system, and Generator *G02* is the slack element of the network model. For the other generators, active power

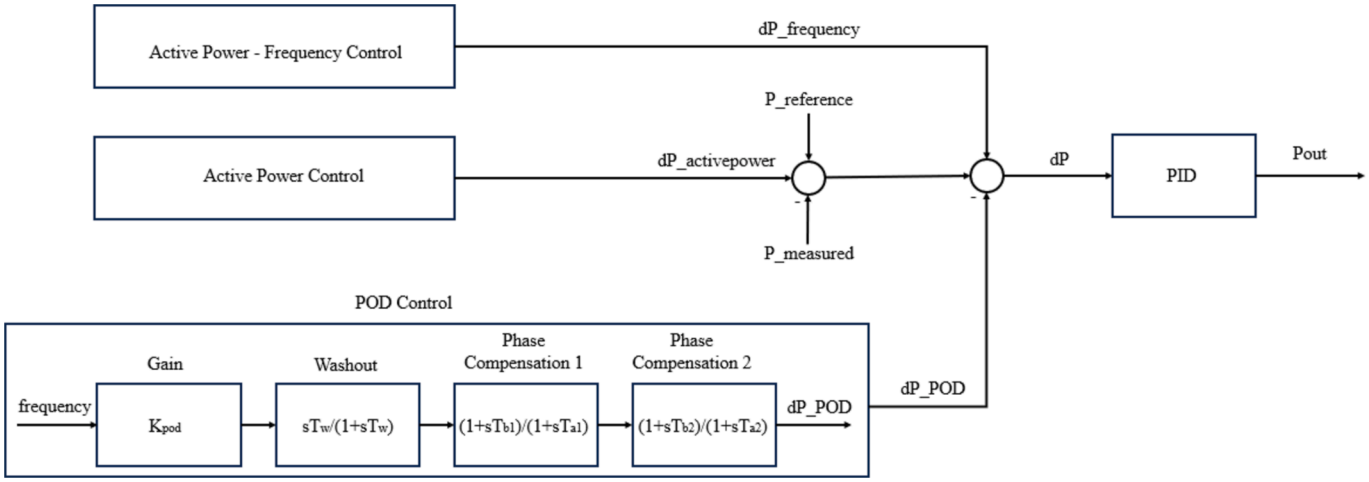

Fig. 2. POD model block diagram

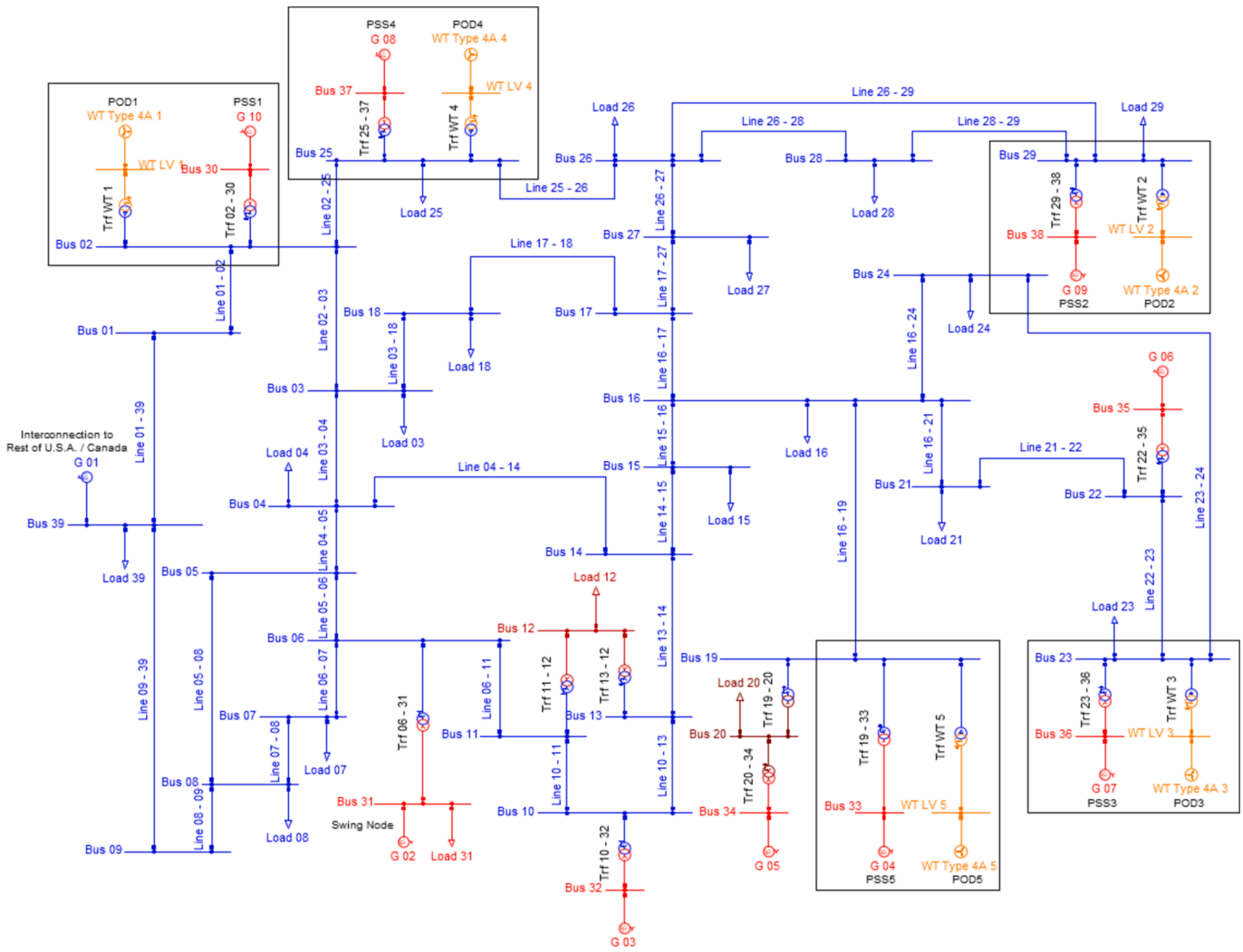

Fig. 3. Modified New England IEEE-39 power system model

dispatch and controlled voltage magnitude at their terminal are given. The data for grid elements, such as generators, loads, transmission lines, and transformers, have been taken from [47].

Regarding the synchronous generator controller, the AVRs used for the synchronous generators in the 39 Bus New England System are rotating excitation systems of IEEE Type 1, according to [47]. Governors are considered as IEEE Type G1(steam turbine) for G02 to G09, and IEEE Type G3 (hydro turbine) for G10. The PSSs are modelled according to [48]. However, the PSS settings given by [48] are not suitable for stabilizing the generator units in the model, because [48] uses different AVR types and settings compared to those used in [47]. No PSS data is given in [47], which is the basis of the DSPF model. Therefore, the PowerFactory model data of the PSSs are entered according to [48], but the PSSs are disabled due to the need for correct parametrization.

The wind turbine controller and wind generator are modeled using the WECC WT Type 4A from the DSPF library.

To study the system's stability, damping controllers are introduced on the generators from the black squares from Fig. 3; wind power plants incorporate a POD-P and POD-Q control, and synchronous generators include a PSS control. Both controls are parameterized appropriately, as explained in Section 5.

The scenarios and results from Sections 4 and 5 indicate the buses, the generators and the controllers associated to each perturbance. To better understand the generation connection and simplify the explanations throughout the article, Table 1 summarizes which terminal each synchronous generator and wind turbine is connected to, indicating the installed damping controller.

Table 1
Terminal connection of synchronous generator and wind turbine

Terminal	Synchronous generator	Wind turbine
Bus 02	G10 (PSS1)	WT1 (POD1)
Bus 06	G02	-
Bus 10	G03	-
Bus 19	G04 (PSS5)	WT5 (POD5)
Bus 20	G05	-
Bus 22	G06	-
Bus 23	G07 (PSS3)	WT3 (POD3)
Bus 25	G08 (PSS4)	WT4 (POD4)
Bus 29	G09 (PSS2)	WT2 (POD2)
Bus 39	G01	-

4. Definition and analysis of the simulation scenarios

The five scenarios defined in this study have been engineered by adjusting lines reactance to generate different initial conditions within DSPF and, therefore, to generate different LFOs in the system. In all scenarios, the same short-circuit of 0.1 ms duration was performed on the same line (*Line 02-03*, Fig. 3). Moreover, the three damping controllers (POD-P, POD-Q and PSS) are disabled in this step of the study.

The study of different LFO scenarios allows for an in-depth examination of the system oscillations in different operating states and the analysis of damping controllers. The scenarios under examination are summarized in Table 2. They can be categorized into three inter-area oscillations, one local oscillation, and a combined oscillation featuring both inter-area and local oscillations. In addition, Table 2 provides a brief description of the generators involved in each oscillation. The scenarios are explained in more detail throughout this Section 4 and divided into time and frequency domain simulations for a better understanding. The comparison between time domain or root main square (RMS) simulation and eigenvalue findings is a robust dual approach that enhances the analysis, providing a more comprehensive understanding of the electromechanical mode. This approach also strengthens the reliability of the scenarios.

4.1. Time domain analysis by root main square simulation

In time domain analysis, frequency and voltage from root main square (RMS) simulation are analyzed at the generation nodes of the modified IEEE-39 network, described in Section 3. The graphs derived from these simulations reveal the intricate interaction between generators, as evidenced by the waveform patterns. Furthermore, the frequency of the oscillations is discernible within these waveforms.

Fig. 4 shows the frequency and voltage graphs from the RMS simulation for all scenarios summarized in Table 2. More specifically, Fig. 4 (a) shows the graphs from *Scenario 1*. In the frequency evolution, Bus 39 oscillates opposite to the rest of the system, having an inter-area oscillation between the area of generator *G01* (*Bus 39*) and the rest of the system's generators with a frequency of 0,269 Hz.

Fig. 4(b) shows the graphs for *Scenario 2*. The waveforms are similar to those of *Scenario 1*. However, in this scenario, the frequency from *Bus 29* has a pronounced contribution to the oscillation, having an inter-area oscillation of frequency 0,261Hz, mainly between the areas of *G01* (*Bus 39*) and *G09* (*Bus 29*).

Fig. 4(c) displays the frequency and voltage graphs from *Scenario 3*. In this plot, finding the oscillation characteristics from the frequency and voltage waveforms is more complicated, and a different representation of this oscillation must be used to find the generators involved in this event. Frequency domain simulation results are provided in Sections 4.2 and 4.3, allowing this oscillation's nature to be analyzed.

Fig. 4(d) shows the frequency and voltage graphs from *Scenario 4*, where a local oscillation of frequency 0.705 Hz is discernible between the area of *G01* (*Bus 39*) and the rest of the system.

Fig. 4(e) shows the frequency and voltage graphs from *Scenario 5*. A combination of inter-area and local oscillations can be seen in the frequency evolution. Regarding the inter-area one, the frequency of *Bus 39* oscillates in opposite to rest of the system, with a frequency of oscillation of 0,576 Hz.

Table 2
Scenarios description

Scenario	Oscillation	Generators involve
1	Inter-area oscillation 1	G01 exhibits inter-area oscillatory behavior in opposition to the whole system
2	Inter-area oscillation 2	G01 exhibits inter-area oscillation against the whole system, with a pronounced contribution from G09
3	Inter-area oscillation 3	G01 shows an inter-area oscillation against the whole system, mainly marked by a phase difference of 180 degrees concerning G05 and G06
4	Local oscillation 1	G01 exhibits local oscillatory behavior in opposition to the whole system
5	Inter-area + Local oscillation 1	G01 shows an inter-area oscillation against to the whole system. At the same time, a local oscillation is identified

4.2. Frequency domain simulation: Eigenvalues

In addition to the time domain graphs, the eigenvalue diagram, from the frequency domain analysis, is a valuable tool for oscillation analysis. It aids in the identification of the system's most critical modes, which are characterized by their minimal damping ratios. In this paper, a threshold of 5% damping ratio, according to the Spanish operating procedure, determines the stability of the system [49]. When all modes exceed this threshold, the system is considered stable. This criterion is particularly important in identifying the modes under investigation, such as the electromechanical mode, which often sets the system's stability boundary and oscillation frequency. Furthermore, the diagram helps in recognizing other system modes that could play a significant role under specific circumstances.

The eigenvalues graph from all scenarios are summarized in Fig. 5. In all scenarios, two modes have been highlighted. *Mode 1* is the mode with a lower damping ratio and is defined as the electromechanical pole, whose frequency matches the oscillation frequency of the RMS diagram, Fig. 5. Moreover, *Mode 2* is also marked because its position can change as the damping controllers are connected, as they influence it. It is worth noting that *Mode 2* may pass to the right of the limit, a phenomenon that is thoroughly explained in Section 5, adding depth to the analysis.

Table 3 summarizes the position for *Mode 1* and *Mode 2* for each scenario. Moreover, the frequency and damping ratio of *Mode 1* are indicated, as it is the most critical mode of the system.

4.3. €Frequency domain simulation: Observability

To further clarify the characteristics of the electromechanical mode (*Mode 1*), the frequency domain analysis includes a polar diagram representing the rotor speed observability factors for synchronous generators. The graphs of all scenarios are summarized in Fig. 6. Arrows within this diagram show the dynamics between synchronous generators, revealing the oscillation interactions between different system zones. This analysis helps to understand RMS simulations better and to conclude which generator zone oscillates against the complex cases with the RMS simulation (Fig. 4). In particular, the time domain simulation results were insufficient to explain *Scenario 3*. However, it can be described using the observability graphs from this section. As shown in Fig. 6(c), the frequency at Bus 39 again oscillates against the entire system, as indicated by angular velocity discrepancies between the generators. Notably, the area of G05 (Bus 20) and G6 (Bus22) are in a phase difference of 180° concerning G01, which defines the main characteristic of the inter-area oscillation with a frequency of 0.22 Hz. This scenario also underscores the significant contribution of the area of G04 (Bus 19) in the oscillation, which, while not precisely a 180° phase difference, has the highest speed observability.

DSPF allows more detailed visualization of the oscillating regions by plotting the rotor speed observability of *Mode 1* on the network. The graphs are summarized in Appendix A.

5. Comparison of the oscillation damping controllers' performance

The five oscillation scenarios described in Section 4 are the starting point for analyzing and comparing the different damping solutions presented in this article. A global initial parameterization has been performed to improve the system's stability in all scenarios by analyzing the participation factor of the state variables. This analysis clarifies the role of each state variable in the oscillatory process and helps to identify the controller parameters with the most significant impact on oscillation damping. The focus is primarily on mitigating inter-area oscillations, identified as the worst-case, with extended efforts to manage local oscillations as feasible, avoiding the search for maximum damping in isolated scenarios in favor of a comprehensive assessment of the adaptability of controllers across a wide range of oscillation scenarios.

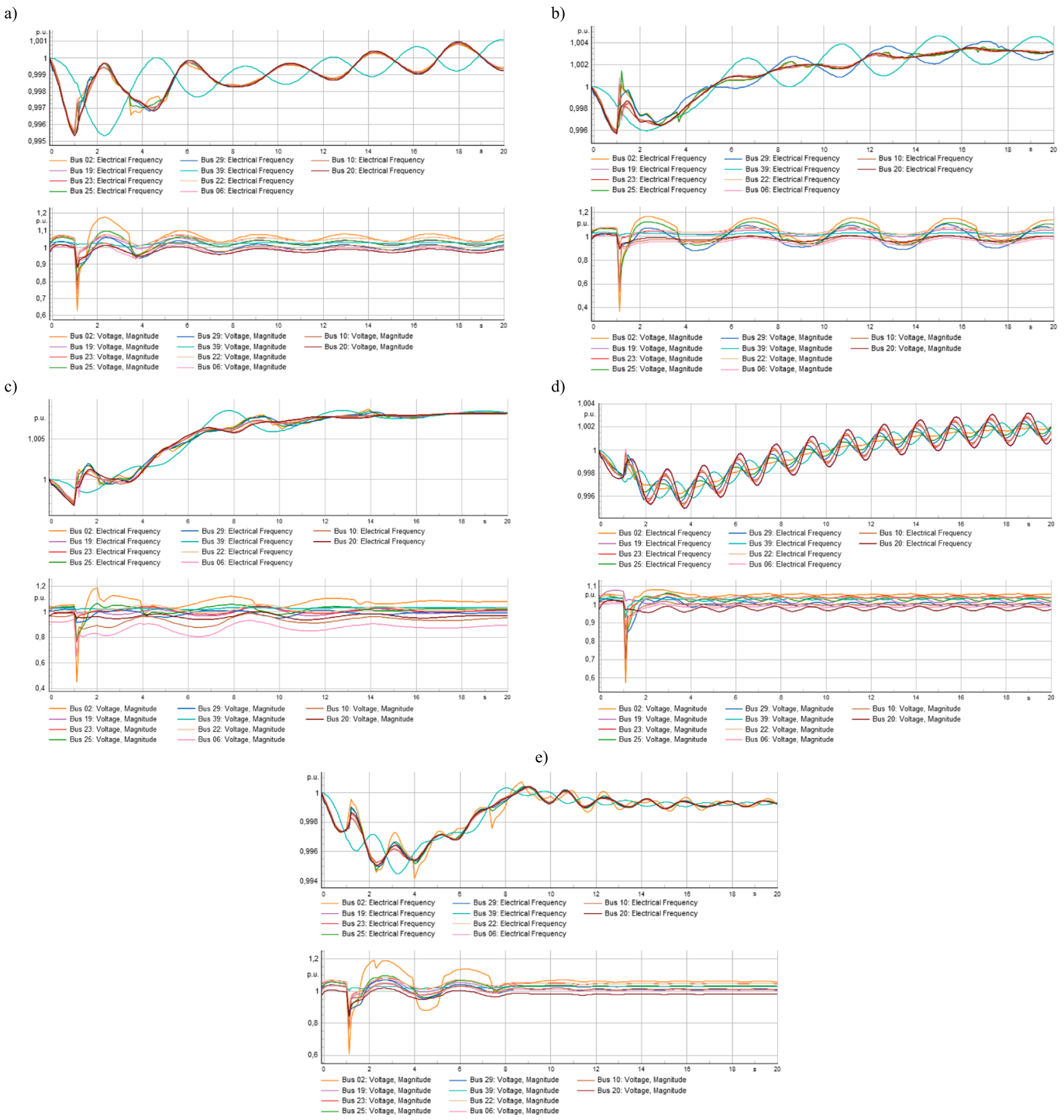

Fig. 4. Time domain simulation: frequency (top plot) and voltage (bottom plot): (a) Scenario 1; (b) Scenario 2; (c) Scenario 3; (d) Scenario 4; (e) Scenario 5.

The steps followed involved adjusting the parameters for the worst-case scenario using a parameter optimization algorithm, based on the participation factor of the state variables of the damping controllers in the electromechanical mode. These parameters were then successively readjusted to ensure they would be effective across all possible scenarios. This research is of utmost importance as it aims to damp these oscillations by employing uniform control parameters in each of the controllers (PSS, POD-P and POD-Q) where possible, and by providing new damping parameters where necessary.

The results have been meticulously and comprehensively analyzed in each scenario, enabling a thorough comparative evaluation of the controllers. For this purpose, POD-P, POD-Q, or PSS controllers are activated individually at each generation node highlighted with the black squares in Fig. 3. In each simulation, only one of the controllers is activated, and it is the same for all the generation nodes of the system. This consistent approach compares the behavior of each type of controller, thereby establishing their versatility and ability to adapt to various oscillation scenarios using a consistent set of parameters.

In addition, the research includes an N-1 contingency analysis for each oscillation analyzed. This procedure simulates the disconnection of the damping controllers one by one to discern their influence on their effectiveness. This aspect of the study aims not only to elucidate the

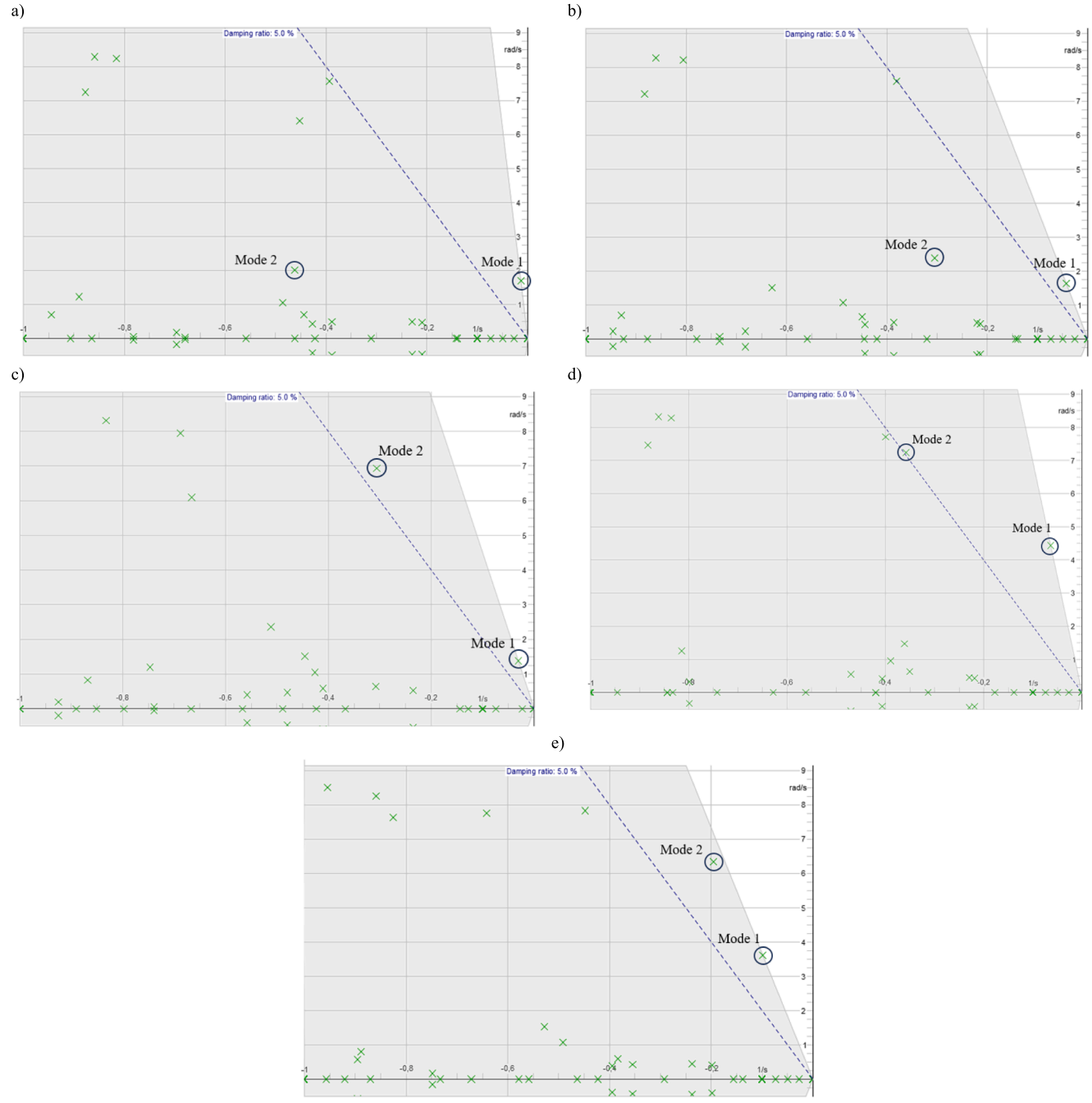

Fig. 5. Eigenvalue diagram: (a) Scenario 1; (b) Scenario 2; (c) Scenario 3; (d) Scenario 4; (e) Scenario 5.

Table 3
Modes description per scenario

Scenario	Oscillation	Mode 1(electromechanical)	Frequency [Hz]	Damping ratio [%]	Mode 2
1	Inter-area oscillation1	-0.014 + 1.689j	0.269	0.82	-0.046 + 2.012j
2	Inter-area oscillation2	-0.043 + 1.644j	0.261	2.62	-0.305 + 2.390j
3	Inter-area oscillation3	-0.031 + 1.384j	0.220	2.23	-0.306 + 6.936j
4	Local oscillation 1	-0.064 + 4.432j	0.705	1.44	-0.358 + 7.237j
5	Inter-area + Local oscillation 1	-0.099 + 3.619j	0.576	2.73	-0.196 + 6.345j

determinants of controller performance but also to uncover possible failure mechanisms, thus improving the operational reliability of damping controllers in practical environments. In addition, the wind resource variability causes uncertainties in energy production and, therefore, in the controller's availability. Thus, the N-1 scenario can approximate a critical case when a power oscillation damping controller is disabled, regardless of the generator production.

At the end of the section, the conclusions and main characteristics of each damping controller obtained from the scenario results are summarized and enumerated.

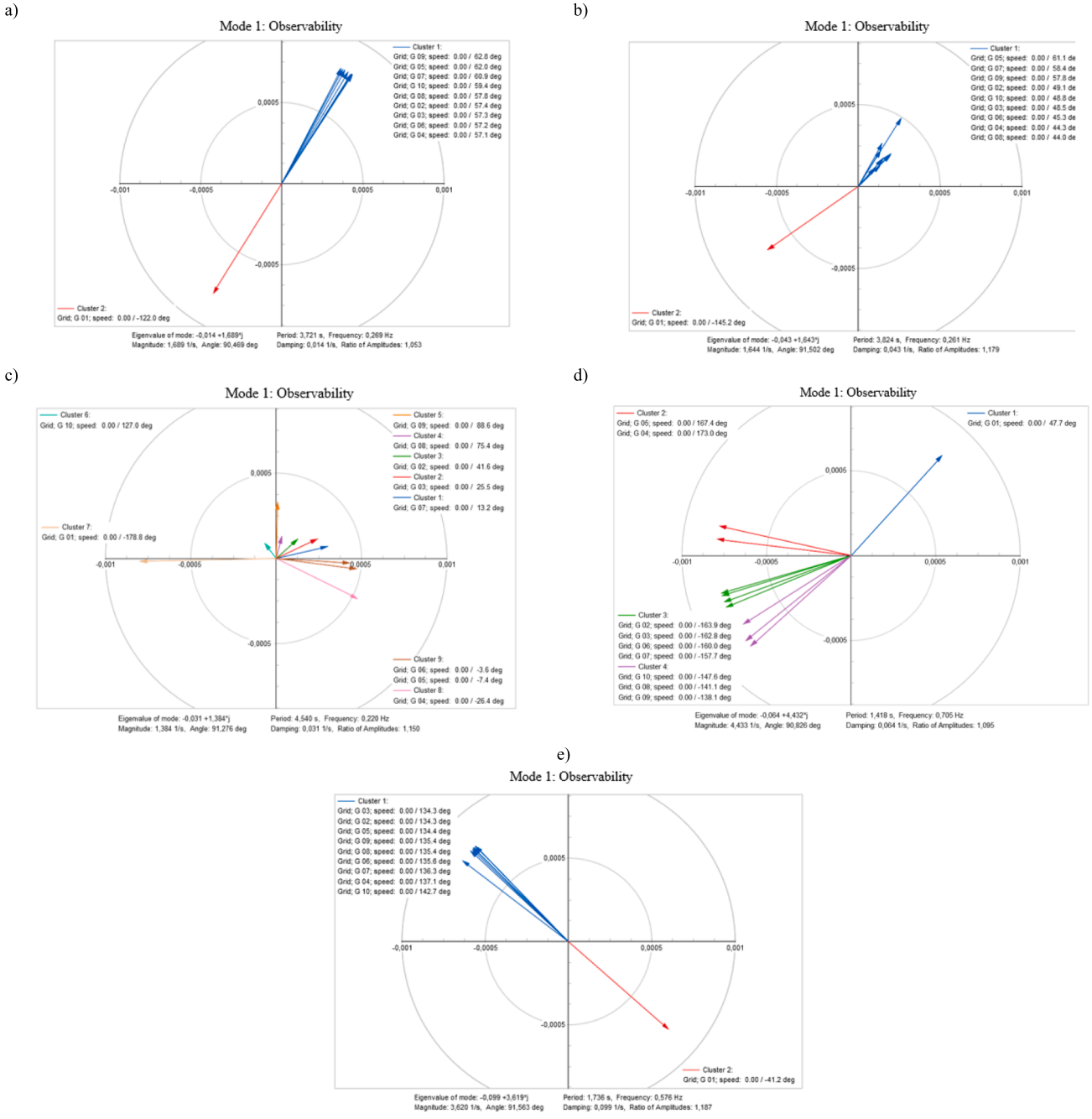

Fig. 6. Polar diagram of the rotor speed observability factors in Mode 1: (a) Scenario 1; (b) Scenario 2; (c) Scenario 3; (d) Scenario 4; (e) Scenario 5.

5.1. Damping controllers results in all scenarios

In this section, two tables for each scenario provide a comprehensive summary of the results evaluation (from Section 5.1.1 to 5.1.5). The first table corresponds to the POD-P, POD-Q, and PSS results, summarized in each row, with "OFF" being the initial condition described in Section 4 when all controllers are disabled. The table summarizes the position in the eigenvalues diagram of each mode and its damping ratio when the controller is activated.

The other table refers to the contingency analysis (N-1) study, wherein the disconnection of each generator's damping controller is methodically simulated to assess the resultant impact on system stability. In this table, "OK," indicates that system stability is assured, and all modes maintain a damping ratio above 5%. Instability is recognized when the removal of a damping controller causes a pole's damping ratio to fall below the 5% threshold, a condition denoted by "NOK" within the table alongside the affected mode.

For an enhanced comprehension of the system's dynamics, each scenario includes a graph representing the state variables with significant participation factors of *Mode 1* and *Mode 2*, indicating each state variable's contribution to the oscillation mode. The most important state variables that appear throughout the section are the following, where *x* represents the generator number indicated in Fig. 3 and Table 1:

- *Grid; G x; psifd*: synchronous generator excitation flux.
- *Grid; G x; speed*: speed of the synchronous generator.
- *Grid; G x; phi*: rotor position angle of the synchronous generator.
- *Power Plant x; AVR x; xf/xe*: state variable of low pass filter of the excitation system.
- *WECC WT Type 4A x; REGC_B; x_lpf_d/x_lpf_q*: state variable of the generator-converter model.
- *PPC x; P/Q CONTROL x; x1*: state variable of the PID of the PPC.

5.1.1. Scenario 1: Inter-area Oscillation 1

Table 4 provides a clear overview of the results of *Scenario 1* when each controller is activated. The data reveals that the activation of any of the three controllers leads to an improvement in the *Mode 1* damping ratio. However, with the POD-Q and PSS controllers, while the stability of *Mode 1* is enhanced, *Mode 2* experiences a decrease in stability due to the significant reduction of the damping ratio, although they do not reach the 5% limit.

Fig. 7 represents the participation factors of *Mode 1* and *Mode 2*. In *Mode 1*, the equality of the bar dimension of the state variables of generators matches the inter-area oscillation detected between the area of generator *G01* and the rest of the system's generators, as no generator has a remarkable participation factor, except *G01* in both modes.

Table 5 presents the results of contingency analysis (N-1), underscoring the system's robustness. Despite the systematic disconnection of each generator's damping controller, the system's overall damping efficacy remains intact. The main reason is that no generator with an oscillation controller significantly contributes to the oscillation.

5.1.2. Scenario 2: Inter-area Oscillation 2

Table 6 details the results of *Scenario 2* when each damping controller is activated. All controllers effectively damp the oscillation, achieving damping coefficients above the 5% threshold. The activation of any of these controllers enhances *Mode 1*'s stability across the evaluated scenarios. However, consistent with the observations in *Scenario 1*, the utilization of POD-Q and PSS, despite increasing *Mode 1*'s stability, detrimentally impacts *Mode 2*'s stability. This effect is more remarkable with the POD-Q controller, which reduces the damping ratio closer to the 5% threshold.

Fig. 8 represents the graph of the participation factors of *Mode 1* and *Mode 2*. *Mode 1* highlights that *G09* and *WT2*, connected to *Bus 29*, display elevated participation levels, indicating the pronounced participation of the area of *Bus 29* in the oscillation.

Table 7 details the N-1 contingency results. Examination of these results reveals that for all evaluated controllers, eliminating the damping controller from Bus 29 (PSS2 or POD2) precipitates system instability, evidenced by *Mode 1*'s damping ratio dropping below the 5% mark. This result indicates the significant engagement of the area of generator *G09* in the oscillatory process, as shown in Fig. 8, exerting a substantial impact on the stability of the electromechanical mode. Additionally, the disconnection of PSS1 results in the destabilization of *Mode 1*, attributed to the considerable influence of *G10*'s voltage on this mode despite its minimal frequency contribution.

5.1.3. Scenario 3 – Inter-area Oscillation 3

Table 8 provides a comprehensive overview of the three damping controllers' effectiveness in addressing this oscillation. Notably, the POD-P controller is the only one that successfully damps the oscillation while maintaining the parameter settings consistent with those employed in *Scenarios 1* and *2*. In contrast, POD-Q and PSS cannot damp the oscillations from this scenario and require meticulous parameter adjustments to achieve damping coefficients above the 5% threshold. In Table 8, the results obtained with this new set of controller parameter is indicated as "*new param. 1*" and are presented in the last two rows of the table. This necessity arises from the substantial variation in the contribution of the generators to the oscillation when compared to the previous scenarios, underscoring the adaptability of the POD-P controller in mitigating the oscillation without parameter readjustment. In contrast, POD-Q and PSS required new parameter tuning, specifically modifications to the lead-lag time constants and gain settings.

Despite the parameter adjustments, PSS struggles to stabilize *Mode 2*. This is evident from the participation factor graph of *Mode 2* (Fig. 9), where the participation factor of generators equipped with PSS is not significantly high, with only *G10* and *WT1* showing elevated participation. This indicates that the contribution of PSS is insufficient to stabilize *Mode 2*, underscoring its limitations in this aspect.

Table 9 provides a summary of the results from the N-1 contingency analysis. Upon careful examination, it becomes evident that the removal of damping controller 1 (POD-P1, POD-Q1, and PSS1) triggers system instability of *Mode 2* across all three controllers. This is due to the high participation factor of *G10* and *WT1*. While these values are not enough to maintain the stability of *Mode 2* under PSS control, they are significant enough to negatively impact the system's stability upon the deactivation of POD-P1 and POD-Q1. Furthermore, the disconnection of damping controller 5 (*Bus 19*) leads to instability in Mode 1 across all evaluated scenarios, highlighting the significant contribution of the area of *Bus 19* in the oscillation.

Table 4
Scenario 1. Results for POD-P, POD-Q, and PSS

Control	Mode 1	Damping ratioMode 1 [%]	Mode 2	Damping ratioMode 2 [%]
OFF	-0.01 + 1.69j	0.82	-0.05 + 2.01j	22.38
POD-P	-0.16 + 1.47j	10.95	-0.70 + 1.54j	41.32
POD-Q	-0.10 + 1.53j	6.45	-0.20 + 2.41j	8.27
PSS	-0.20 + 1.63j	11.93	-0.20 + 2.04j	9.71

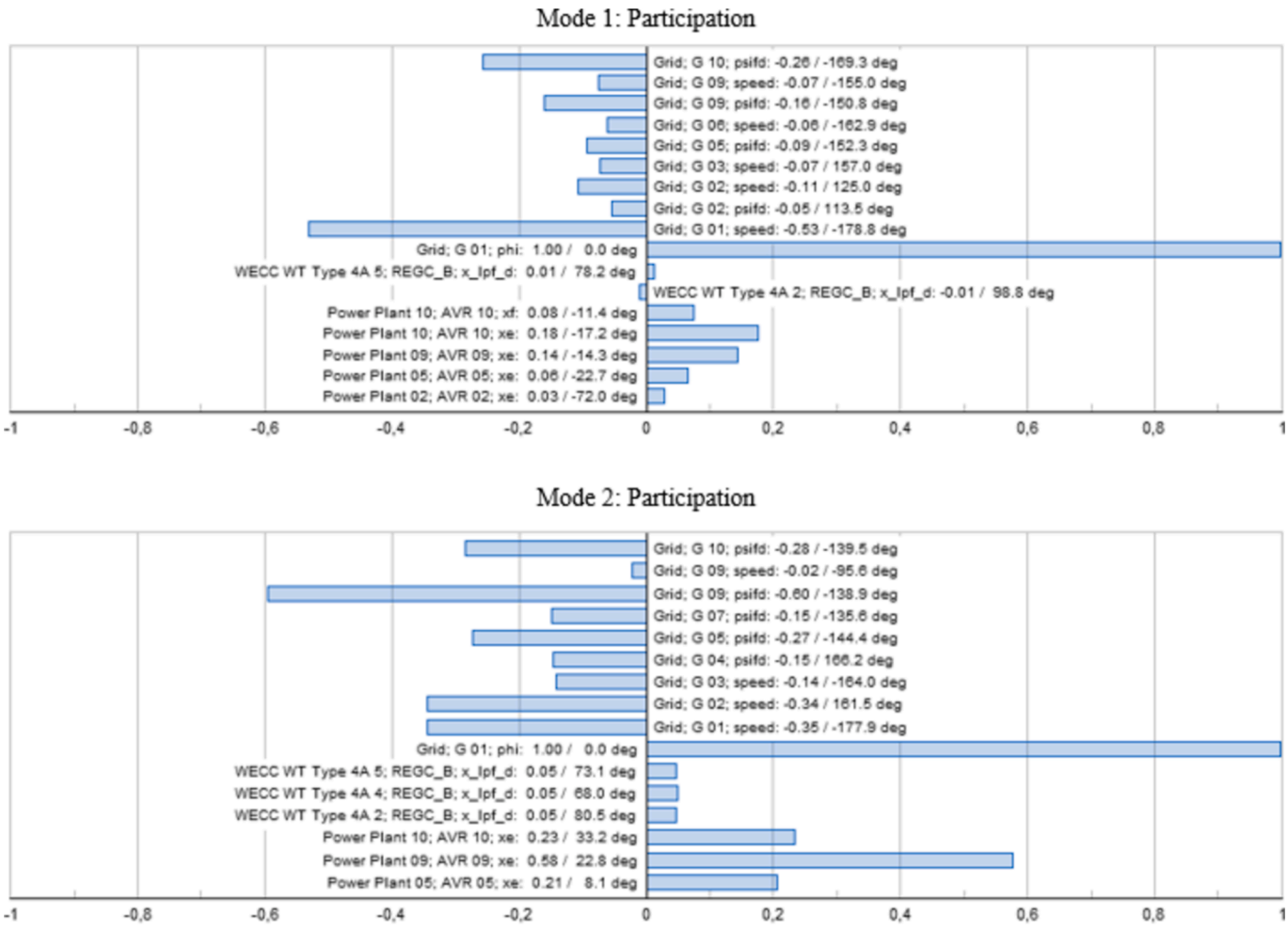

Fig. 7. Scenario 1. Participation Factor bar plot for Mode1 and Mode2

Table 5
Scenario 1. Results for POD-P, POD-Q, and PSS in N-1 scenario

Control	Losing PSS1/ POD1	Losing PSS2/ POD2	Losing PSS3/ POD3	Losing PSS4/ POD4	Losing PSS5/ POD5
POD-P	OK	OK	OK	OK	OK
POD-Q	OK	OK	OK	OK	OK
PSS	OK	OK	OK	OK	OK

5.1.4. *Scenario 4 – Local Oscillation 1*

Table 10 presents a comparative analysis of the three damping controllers. As in *Scenario 3*, due to substantial shifts in generator contributions to the oscillation, only the POD-P controller successfully damp the oscillation, maintaining the initial parametrization from *Scenario 1* and *2*. POD-Q and PSS not only do not improve, but worsen the damping ratio and require reparameterization to achieve effective oscillation damping, indicated as '*new param. 2*' in the table.

As in *Scenario 3*, despite adjustments, PSS still fails to stabilize *Mode 1*. This is due to the poor participation factors among generators equipped with PSS, as detailed in the participation factor graph of Fig. 10.

Table 11 shows the N-1 contingency analysis. Notably, the analysis reveals that *Mode 1* becomes unstable with the loss of POD-P3. Similarly, the system becomes unstable upon the loss of POD-Q2. The POD-Q instability is a direct consequence of the significant role of the area of generator *G09* involved in the oscillation. The loss of POD-P3, despite this controller's similar behavior to other generators and no distinct oscillatory behavior, precipitates instability in *Mode 1*. This is because the controller is initially optimized to damp inter-area rather than local oscillations, highlighting the critical nature of parameter optimization. The authors tested that fine-tuning the parameters and conducting the N-1 analysis in scenarios involving the loss of a POD-P controller resulted in all modes achieving stability, underscoring the importance of precise parameterization to ensure system resilience.

Table 6
Scenario 2. Results for POD-P, POD-Q, and PSS

Control	Mode 1	Damping ratio 1 [%]	Mode 2	Damping ratio 2 [%]
OFF	-0.04 + 1.64j	2.62	-0.31 + 2.39j	12.67
POD-P	-0.10 + 1.55j	6.73	-0.51 + 1.79j	27.66
POD-Q	-0,08 + 1.57j	5.37	-0.16 + 2.54j	6.32
PSS	-0.08 + 1.62j	5.20	-0.26 + 2.46j	10.62

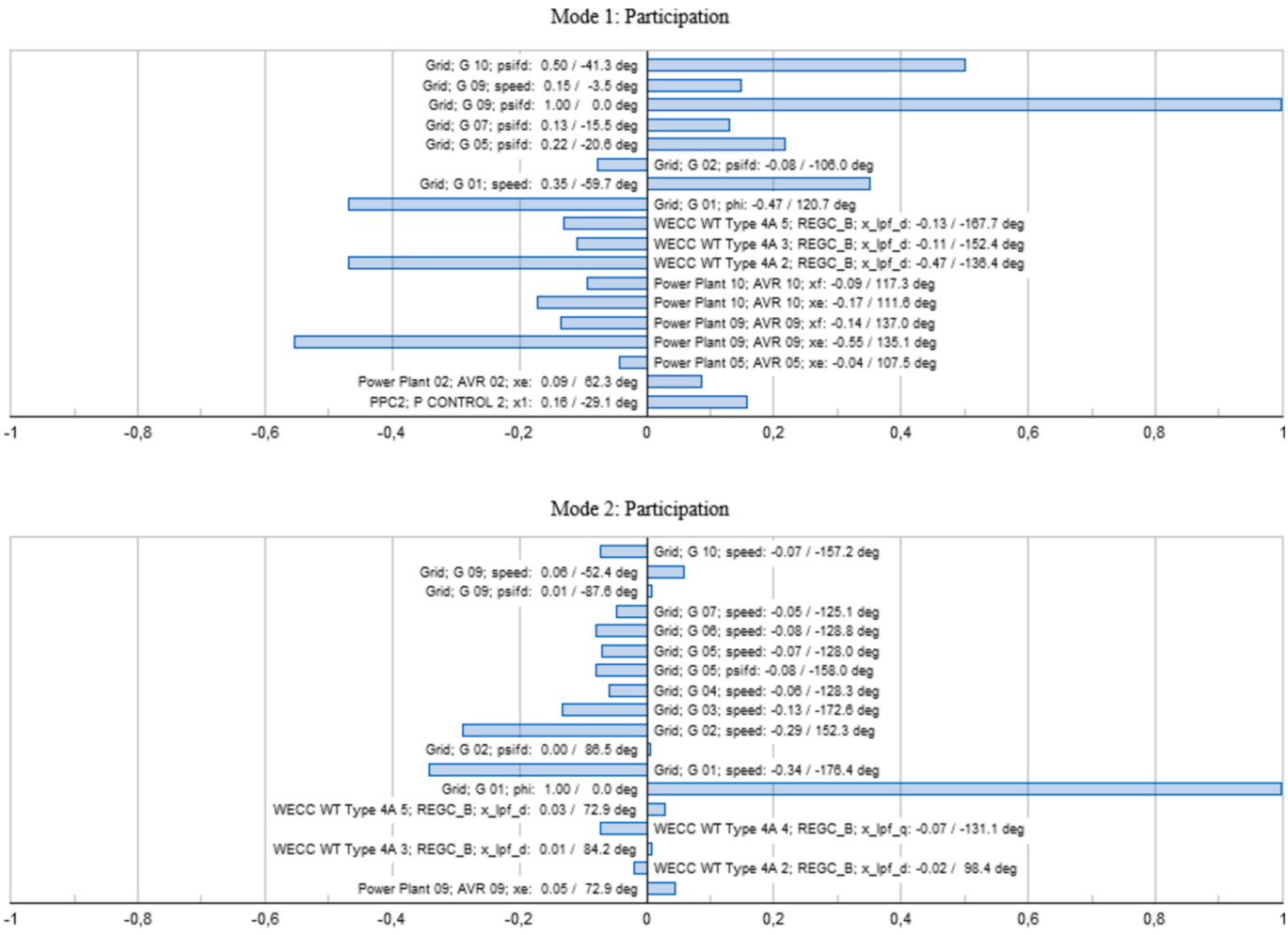

Fig. 8. Scenario 2. Participation Factor bar plot for Mode1 and Mode2

Table 7
Scenario 2. Results for POD-P, POD-Q, and PSS in N-1 scenario

Control	Losing PSS1/POD1	Losing PSS2/POD2	Losing PSS3/POD3	Losing PSS4/POD4	Losing PSS5/POD5
POD-P	OK	NOK (Mode 1)	OK	OK	OK
POD-Q	OK	NOK (Mode 1)	OK	OK	OK
PSS	NOK (Mode 1)	NOK (Mode 1)	OK	OK	OK

5.1.5. Scenario 5 –Inter-area and local oscillation 1

Table 12 provides a clear overview of the results of *Scenario 5* when each controller is activated. After evaluating the results, it is confirmed that the POD-P is the only one capable of damping oscillation while maintaining parameter consistency across all evaluated scenarios. Due to significant shifts in generator contributions to the oscillation, the POD-Q controller must recalibrate parameters to achieve effective oscillation damping, indicated as '*new param. 3*'. Conversely, the PSS configuration has been retained from the local oscillation parameters in *Scenario 4*.

Despite reparameterization for PSS, *Mode 1* remains unstable, indicating the need for participation factors in the generators equipped with PSS in the oscillation (Fig. 11). The insufficiency of PSS's contribution to stabilize *Mode 1* highlights again a significant limitation in PSS's effectiveness.

The N-1 contingency analysis is summarized in Table 13. Conversely, the deactivation of any POD-Q controller does not precipitate instability, which is attributable to the absence of any single generator exhibiting dominant participation in the oscillation. Notably, within the POD-P configuration, *Mode 2* transitions to instability upon the loss of POD-P1. This instability reproduces the situation in *Scenario 4*, where the controller is primarily optimized to address inter-area oscillations rather than local oscillations.

5.2. Discussion and main characteristics of the damping controllers analysis

The following general characteristics can be extracted from the results obtained from *Scenario 1* to *Scenario 5*:

1. The PSS demonstrates the ability to damp not only local oscillations, but also inter-area oscillations, dependent on correct parameterization.
2. Activation of the POD-Q and PSS controllers to stabilize a specific electromechanical mode may unintentionally decrease the stability of other system modes.

Table 8
Scenario 3. Results for POD-P, POD-Q, and PSS

Control	Mode 1	Damping ratio 1 [%]	Mode 2	Damping ratio 2 [%]
OFF	-0.03 + 1,38j	2,23	-0.31 + 6,93j	4.41
POD-P	-0.07 + 1.37j	5.42	0.36 + 6.90j	5.22
POD-Q	-0.03 + 1.39j	2.24	-0.31 + 6.93j	4.49
PSS	-0.02 + 1.37j	1.75	-0.31 + 6.95j	4.42
POD-Q (new param.1)	-0.11 + 1.37j	8.21	-0.36 + 6.90j	5.15
PSS (new param.1)	-0.08 + 1.36	5.75	-0.31 + 6.95	4.45

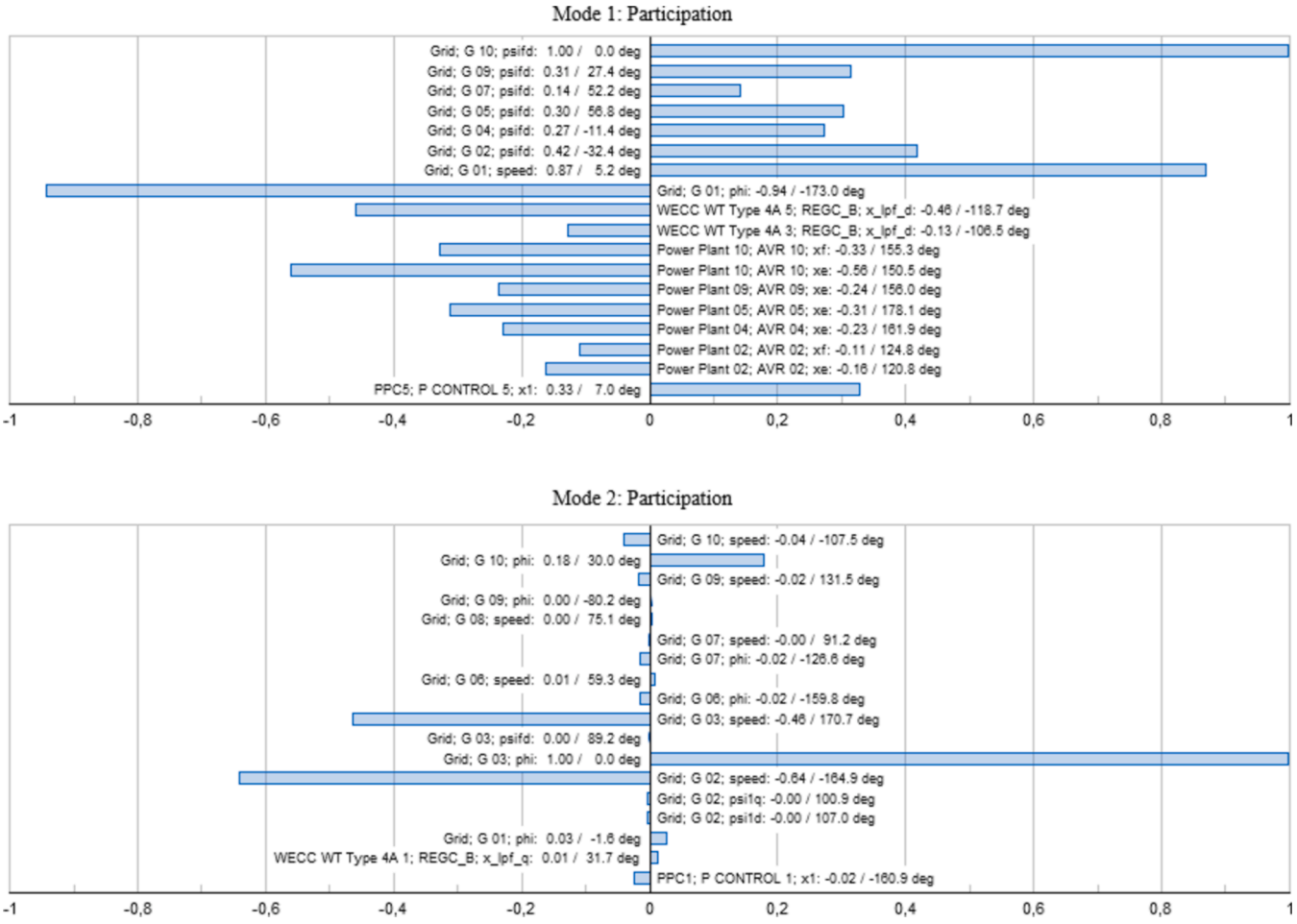

Fig. 9. Scenario 3. Participation Factor bar plot for Mode1 and Mode2

Table 9
Scenario 3. Results for POD-P, POD-Q, and PSS in N-1 scenario

Control	Losing PSS1/POD1	Losing PSS2/POD2	Losing PSS3/POD3	Losing PSS4/POD4	Losing PSS5/POD5
POD-P	NOK (Mode 2)	OK	OK	OK	NOK (Mode 1)
POD-Q	NOK (Mode 2)	OK	OK	OK	NOK (Mode 1)
PSS	NOK (Mode 2)	NOK (Mode 2)	NOK (Mode 2)	NOK (Mode 2)	NOK (Mode 1, 2)

Table 10
Scenario 4. Results for POD-P, POD-Q, and PSS

Control	Mode 1	Damping ratio 1 [%]	Mode 2	Damping ratio 2 [%]
OFF	-0.064 + 4.43j	1.44	-0.358 + 7.24j	4.94
POD-P	-0.39 + 4.39j	8.84	-0.39 + 7.30j	5.04
POD-Q	-0.06 + 4.47j	1.29	0.37 + 7.24j	5.09
PSS	-0.06 + 4.48j	1.25	0.33 + 7.34j	0.33
POD-Q (new param. 2)	-0.25 + 4.60j	5.52	-0.25 + 4.60j	5.52
PSS (new param. 2)	-0.06 + 4.50j	1.31	-0.44 + 7.73j	5.66

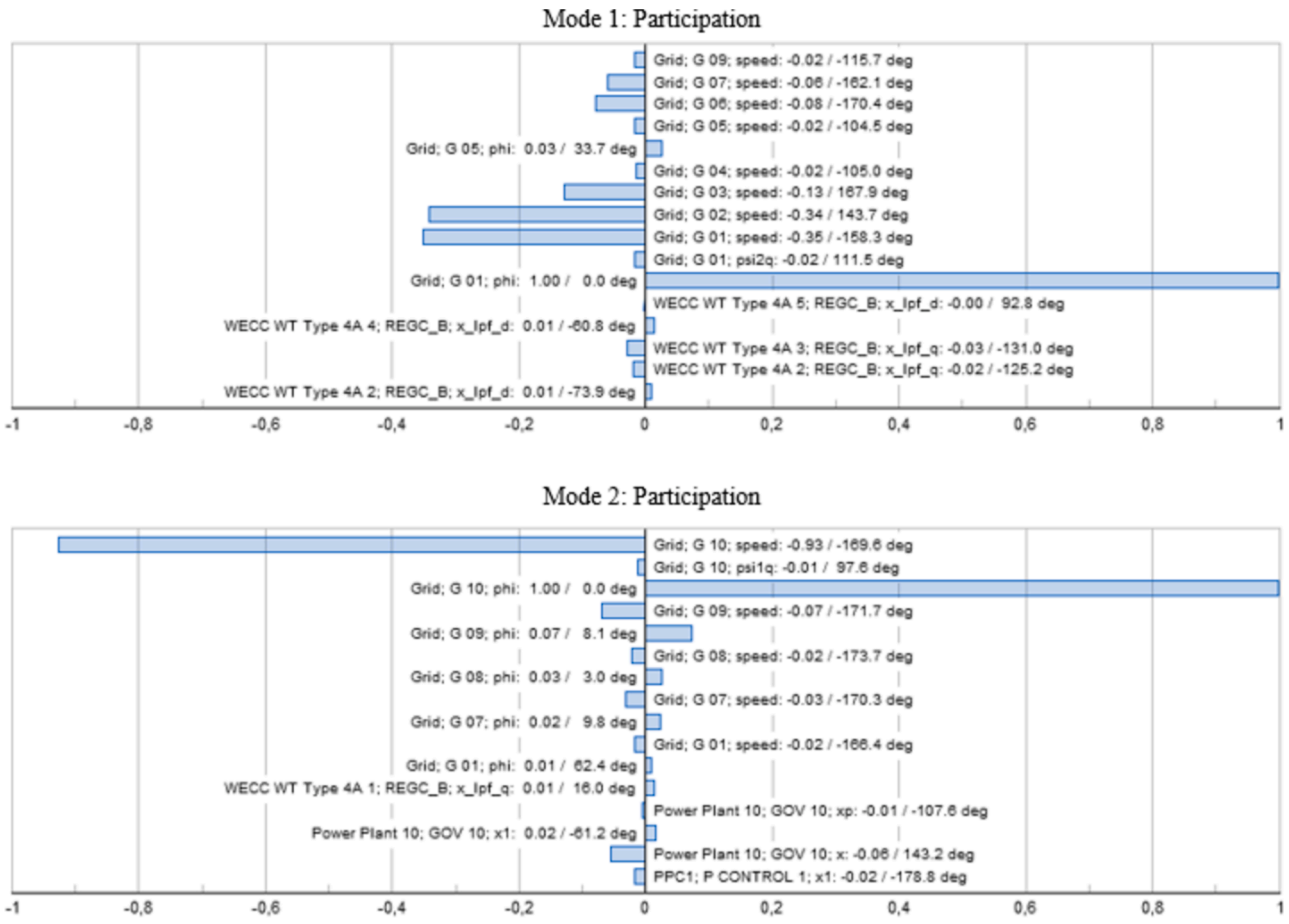

Fig. 10. Scenario 4. Participation Factor bar plot for Mode1 and Mode2

Table 11
Scenario 4. Results for POD-P, POD-Q, and PSS in N-1 scenario

Control	Losing PSS1/POD1	Losing PSS2/POD2	Losing PSS3/POD3	Losing PSS4/POD4	Losing PSS5/POD5
POD-P	OK	OK	NOK (Mode 1)	OK	OK
POD-Q	OK	NOK (Mode 1)	OK	OK	OK
PSS	NOK (Mode 1)	NOK (Mode 1)	NOK (Mode 1)	NOK (Mode 1)	NOK (Mode 1)

Table 12
Scenario 5. Results for POD-P, POD-Q and PSS

Control	Mode 1	Damping ratio 1 [%]	Mode 2	Damping ratio 2 [%]
OFF	-0.10 + 3.62j	2.73	-0.20 + 6.35j	3.08
POD-P	-0.95 + 4.26j	21.78	-0.44 + 6.68j	6.55
POD-Q	-0.07 + 3.76j	1.78	-0.21 + 6.37j	3.29
PSS	-0.07 + 3.67j	1.86	-0.18 + 6.36j	2.76
POD-Q (new param. 3)	-0.51 + 2.98j	16.77	-0.38 + 6.41j	5.99
PSS (new param.2)	-0.07 + 3.83j	1.92	-0.46 + 6.91j	6.62

3. System stability remains largely unaffected by the disengagement of a damping controller unless it is directly associated with a generator that is actively oscillating against the system.
4. Elevated participation factors in the electromechanical mode indicate that generators exhibit significant engagement in oscillatory dynamics. Consequently, the loss of such generator controllers can sustain the mode within the unstable region of the eigenvalue diagram, identified by a damping ratio below 5%.
5. PSS's impact on a mode is not solely contingent on its frequency (speed) contribution; a substantial voltage contribution can equally exert a strong influence on mode stability.
6. Among the evaluated controllers, the POD-P stands out as the most efficacious in damping oscillations across a broader range of generator participation scenarios. Therefore, POD-P is the recommended controller for oscillation damping. Conversely, the efficacy of POD-Q and PSS depends on the specific generators' contribution and the characteristic of the oscillation.

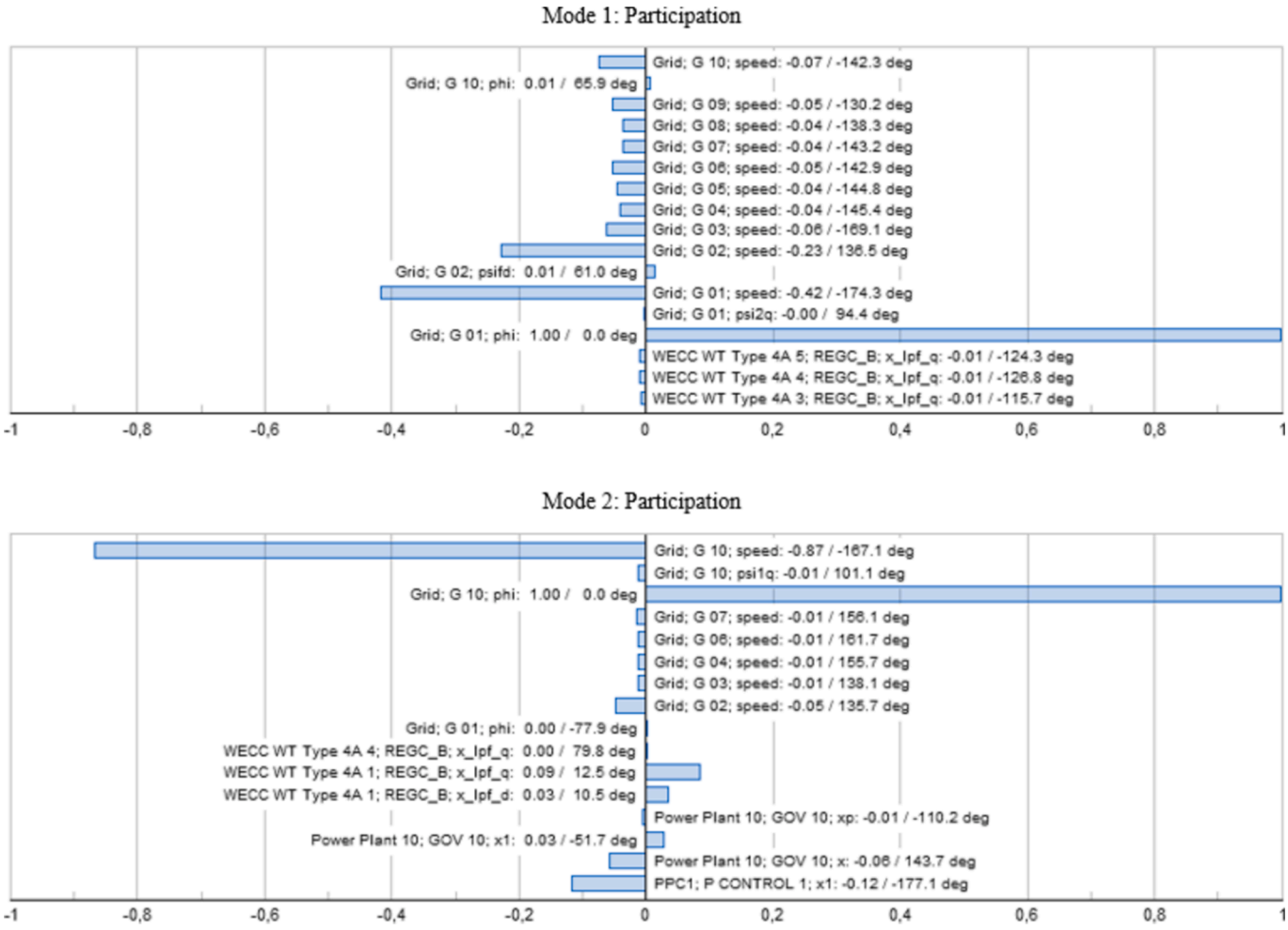

Fig. 11. Scenario 5. Participation Factor bar plot for Mode1 and Mode2

Table 13
Scenario 5. Results for POD-P, POD-Q, and PSS in N-1 scenario

Control	Losing PSS1/POD1	Losing PSS2/POD2	Losing PSS3/POD3	Losing PSS4/POD4	Losing PSS5/POD5
POD-P	NOK (Mode 1)	OK	OK	OK	OK
POD-Q	OK	OK	OK	OK	OK
PSS	NOK (Mode 1,2)	NOK (Mode 1)	NOK (Mode 1)	NOK (Mode 1)	NOK (Mode 1)

7. In instances where generators equipped with PSS do not have a participation factor in the oscillation, the stability of the system mode is compromised regardless of the PSS parameter settings due to the PSS's lack of influence on the oscillatory mode.
8. The versatility of the POD-P controller is challenged by the loss of a controller, attributed to its optimization needing to be specifically tailored. This could lead to instability in a mode previously considered stable, triggered by the removal of a generator perceived to have minimal influence on the oscillation dynamics.

6. Conclusion

The comprehensive study presented in this paper delves into the performance and adaptability of PSS, POD-P, and POD-Q power strategies in various oscillatory scenarios of an integrated power system with renewables. The objective has been to analyze individually the behavior, strengths, and weaknesses of each damping controller and its versatility under different oscillations. Through simulations performed with DIgSILENT PowerFactory and a modified IEEE 39 Bus New England System model, the research provided an in-depth analysis of the effectiveness of the controllers in damping local and inter-area oscillations under different grid conditions.

The comprehensive analysis of damping controllers across various scenarios in a renewable-integrated power system has yielded several significant insights regarding the performance and applicability of PSS, POD-P, and POD-Q controllers. PSS effectively damps inter-area oscillations with proper parameterization, but both PSS and POD-Q may inadvertently reduce the stability of other system modes when activated. System stability typically remains unaffected by the disengagement of a damping controller unless it is directly connected to a critical, oscillating generator. Among the controllers, POD-P stands out for its superior ability to manage oscillations across various scenarios, making it the most adaptable and effective choice. However, the utility of POD-P is challenged if a controller is lost, particularly in non-optimally parameterized systems, indicating the need for finely tuned, adaptive control strategies. The effectiveness of POD-Q and PSS is also notably contingent on the specific generators involved in the oscillations, highlighting the importance of strategic controller placement and settings aligned with generator dynamics. These insights underscore the complexities of deploying advanced damping controls and the need to consider generator characteristics and system dynamics in controller configuration carefully.

The study highlights the need for further controller design and system modelling research, mainly through more comprehensive and complex network models that include a wide range of RES types and configurations. In addition, exploring the potential for new FACTS device types and hybrid controller strategies could further improve system resilience and efficiency.

In conclusion, this research confirms that the strategic application of PSS, POD-P, and POD-Q controllers, configured and optimized based on specific system requirements, can significantly improve the damping of oscillations and, thereby, the overall stability of renewable-rich power systems. These insights are vital for power system operators and planners seeking to enhance grid reliability and performance in the face of increasing renewable energy integration. This study not only contributes to the theoretical understanding of damping control in power systems but also provides practical guidelines for the deployment and operation of these critical stability-enhancing technologies.

CRediT authorship contribution statement

Marta Bernal-Sancho: Writing – review & editing, Writing – original draft, Software, Methodology, Investigation, Formal analysis, Data curation, Conceptualization. **María Paz Comech:** Writing – review & editing, Supervision. **Noemí Galán-Hernández:** Writing – review & editing, Supervision.

Declaration of competing interest

The authors declare that they have no known competing financial interests or personal relationships that could have appeared to influence the work reported in this paper.

Data availability

The authors do not have permission to share data.

Acknowledgements

This work has been funded by the European Union's Horizon Europe Energy Research and Innovation program under the project eFORT (Grant Agreement no. 101075665). The content of the article reflects the views only of the authors. The European Commission is not re-sponsible for any use that may be made of the information contained therein.

Appendix. Eigenvalues complementary graphs

Fig. 12 shows the rotor speed observability factors for *Mode 1* in the network diagram for all scenarios. This helps to identify the specific generators involved in the oscillation, corroborating the RMS simulation findings, and helping to understand polar plots of Fig. 6.

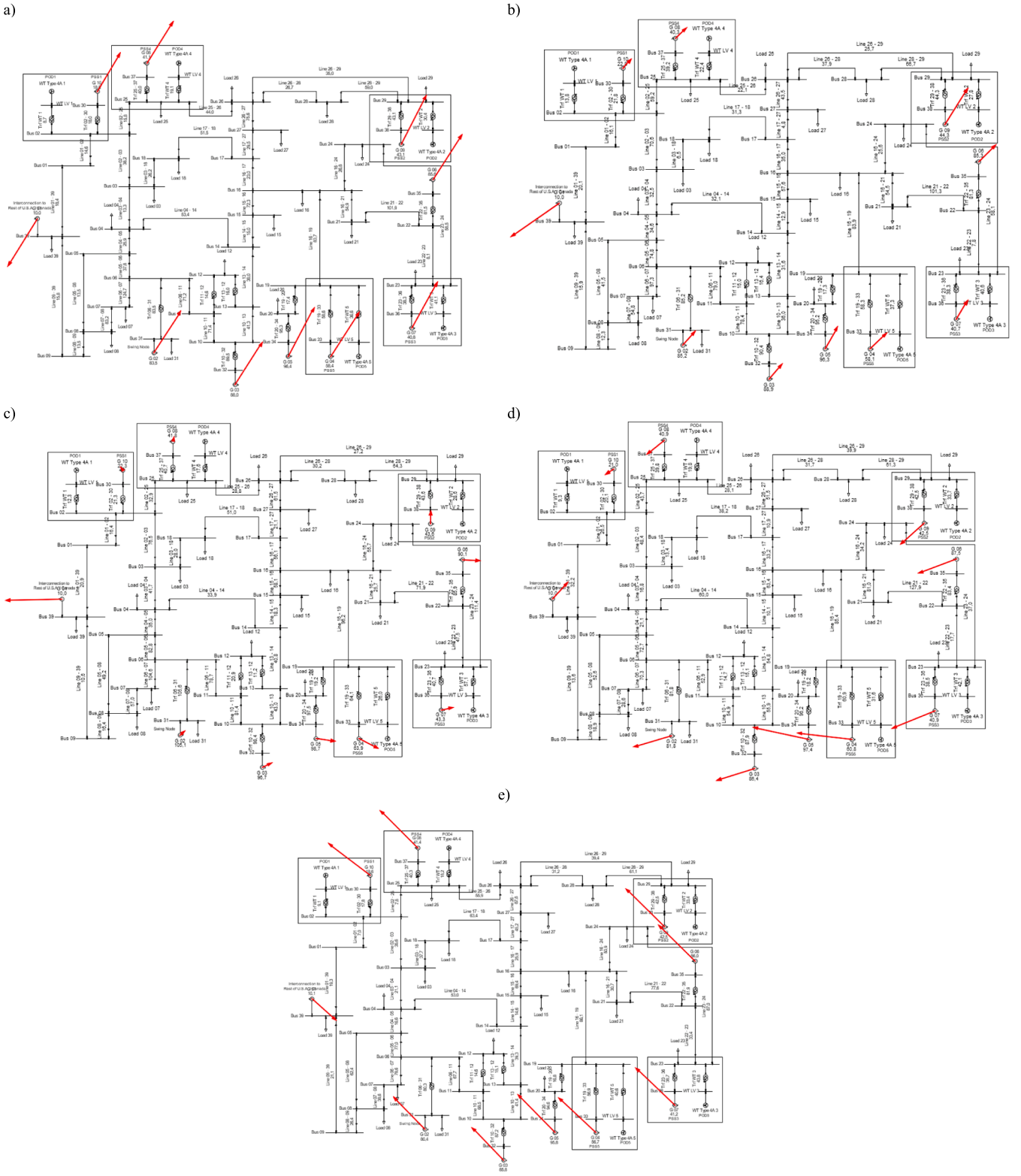

Fig. 12. Rotor speed observability factors for Mode 1 in the network diagram: (a) Scenario 1; (b) Scenario 2; (c) Scenario 3; (d) Scenario 4; (e) Scenario 5.

References

[1] A. Adrees, P.N. Papadopoulos, J.V. Milanovic, A framework to assess the effect of reduction in inertia on system frequency response, en *2016 IEEE Power and Energy Society General Meeting (PESGM)*, Boston, MA, USA: IEEE, jul. 2016, pp. 1-5. doi: 10.1109/PESGM.2016.7741695.

[2] M.I. Saleem, S. Saha, T.K. Roy, S.K. Ghosh, Assessment and management of frequency stability in low inertia renewable energy rich power grids, *IET Generation Trans & Dist*, p. gtd2.13129, feb. 2024, doi: 10.1049/gtd2.13129.

[3] Garmroodi M, Hill DJ, Verbic G, Ma J. Impact of tie-line power on inter-area modes with increased penetration of wind power. IEEE Trans. Power Syst. 2016;31(4): 3051–9. https://doi.org/10.1109/TPWRS.2015.2477536.

[4] Kumar A, et al. Optimized robust control for improving frequency response of delay dependent AC microgrid with uncertainties. Electr. Pow. Syst. Res. 2024;229: 110138. https://doi.org/10.1016/j.epsr.2024.110138.

[5] Prabha Kundur, *Power System Stability and Control.pdf*, McGraw-Hill. Palo Alto, California: 0-07-035958-X, 1994.

[6] Xiong L, et al. Optimal allocation and sizing of ESSs for power system oscillation damping under high wind power penetration. Int. J. Electr. Power Energy Syst. 2023;153:109385. https://doi.org/10.1016/j.ijepes.2023.109385.

[7] He P, Fang Q, Jin H, Ji Y, Gong Z, Dong J. Coordinated design of PSS and STATCOM-POD based on the GA-PSO algorithm to improve the stability of wind-PV-thermal-bundled power system. Int. J. Electr. Power Energy Syst. 2022;141: 108208. https://doi.org/10.1016/j.ijepes.2022.108208.

[8] A. Aghazade, A. Kazemi, Simultaneous coordination of power system stabilizers and STATCOM in a multi-machine power system for enhancing dynamic performance, en *2010 4th International Power Engineering and Optimization Conference (PEOCO)*, Shah Alam, Selangor, Malaysia: IEEE, jun. 2010, pp. 13-18. doi: 10.1109/PEOCO.2010.5559221.

[9] Mahdiyeh. Eslami, Hussain. Shareef, y Azah. Mohamed, «Coordinated design of PSS and TCSC controller for power system stability improvement», en *2010 Conference Proceedings IPEC*, Singapore, Singapore: IEEE, oct. 2010, pp. 433-438. doi: 10.1109/IPECON.2010.5697035.

[10] S. Mahapatra, A.N. Jha, PSS & TCSC coordinated design using particle swarm optimization for power system stability analysis, en *2012 2nd International Conference on Power, Control and Embedded Systems*, Allahabad, Uttar Pradesh, India: IEEE, dic. 2012, pp. 1-5. doi: 10.1109/ICPCES.2012.6508094.

[11] Cai LJ, Erlich I. Simultaneous Coordinated Tuning of PSS and FACTS Damping Controllers in Large Power Systems. IEEE Trans. Power Syst. 2005;20(1):294–300. https://doi.org/10.1109/TPWRS.2004.841177.

[12] Hasanvand H, Arvan MR, Mozafari B, Amraee T. Coordinated design of PSS and TCSC to mitigate interarea oscillations. Int. J. Electr. Power Energy Syst. 2016;78: 194–206. https://doi.org/10.1016/j.ijepes.2015.11.097.

[13] Tripathy M, Mishra S. Coordinated tuning of PSS and TCSC to improve Hopf Bifurcation margin in multimachine power system by a modified Bacteria Foraging Algorithm. Int. J. Electr. Power Energy Syst. 2015;66:97–109. https://doi.org/10.1016/j.ijepes.2014.10.022.

[14] Khodabakhshian A, Esmaili MR, Bornapour M. Optimal coordinated design of UPFC and PSS for improving power system performance by using multi-objective water cycle algorithm. Int. J. Electr. Power Energy Syst. 2016;83:124–33. https://doi.org/10.1016/j.ijepes.2016.03.052.

[15] Furini MA, Pereira ALS, Araujo PB. Pole placement by coordinated tuning of Power System Stabilizers and FACTS-POD stabilizers. Int. J. Electr. Power Energy Syst. 2011;33(3):615–22. https://doi.org/10.1016/j.ijepes.2010.12.019.

[16] R.F. Mochamad, S.P. Hadi, B.S.M. Isnaeni, «TVAC PSO for modal optimal control POD and PSS coordination in UPFC», en *2014 6th International Conference on Information Technology and Electrical Engineering (ICITEE)*, Yogyakarta, Indonesia: IEEE, oct. 2014, pp. 1-6. doi: 10.1109/ICITEED.2014.7007951.

[17] R. Visakhan, R. Rahul, A.A. Kurian, Comparative study of PSS and FACTS-POD for power system performance enhancement, en *2015 International Conference on Power, Instrumentation, Control and Computing (PICC)*, Thrissur, India: IEEE, dic. 2015, pp. 1-6. doi: 10.1109/PICC.2015.7455768.

[18] R. Visakhan, A. A. Kurian, S. Sreedharan, «Comparative study of PSS and STATCOM-POD for Transient Stability in Microgrid, *Asian Journal of Engineering and Technology*, vol. 03, 04.

[19] Mithulananthan N, Canizares CA, Reeve J, Rogers GJ. Comparison of PSS, SVC, and STATCOM controllers for damping power system oscillations. IEEE Trans. Power Syst. 2003;18(2):786–92. https://doi.org/10.1109/TPWRS.2003.811181.

[20] Prakash A, Moursi MSE, Parida SK, Kumar K, El-Saadany EF. Damping of Inter-Area Oscillations With Frequency Regulation in Power Systems Considering High Penetration of Renewable Energy Sources. IEEE Trans. on Ind. Applicat. 2024;60 (1):1665–79. https://doi.org/10.1109/TIA.2023.3312061.

[21] Kumar A, Bhadu M. Wide-area damping control system for large wind generation with multiple operational uncertainty. Electr. Pow. Syst. Res. 2022;213. https://doi.org/10.1016/j.epsr.2022.108755.

[22] «COMMISSION REGULATION (EU) 2016/ 631 - of 14 April 2016 - establishing a network code on requirements for grid connection of generators».

[23] «European Union Agency for the Cooperation of Energy Regulators», ACER. [En línea]. Disponible en: https://www.acer.europa.eu/electricity/connection-codes.

[24] REE, aelec, ufd Grupo Naturgy, cide, Aseme, «Norma técnica de supervisión de la conformidad de los módulos de generación de electricidad según el Reglamento UE 2016/631», 9 de julio de 2021.

[25] FINGRID, «Specific study requirements for power park modules related to risk of subsynchronous oscillations», feb. 2022.

[26] Australian Energy Market Commission, South Australian Minister, «National Electricity Rules Version 204», dic. 2023.

[27] Tang Z, Hill DJ, Liu T, Song Y. Distributed inter-area oscillation damping control for power systems by using wind generators and load aggregators. Int. J. Electr. Power Energy Syst. 2020;123:106201. https://doi.org/10.1016/j.ijepes.2020.106201.

[28] T. Surinkaew, I. Ngamroo, Two-level robust coordinated stabilizing control of PSS and DFIG wind turbine for enhancing grid resiliency, en *2016 Power Systems Computation Conference (PSCC)*, Genoa, Italy: IEEE, jun. 2016, pp. 1-7. doi: 10.1109/PSCC.2016.7540935.

[29] P. Jaengarun, S. Tiptipakorn, T. Singhavilai, Comparative Study of PSS and POD for A Power System With PV Plant, en *2020 International Conference on Power, Energy and Innovations (ICPEI)*, Chiangmai, Thailand: IEEE, oct. 2020, pp. 169-172. doi: 10.1109/ICPEI49860.2020.9431424.

[30] Nikolaev N, Dimitrov K, Rangelov Y. A Comprehensive Review of Small-Signal Stability and Power Oscillation Damping through Photovoltaic Inverters. Energies 2021;14(21):7372. https://doi.org/10.3390/en14217372.

[31] Li M, Xiong L, Chai H, Xiu L, Hao J. Mechanism of PV generation system damping electromechanical oscillations. IEEE Access 2020;8:135853–65. https://doi.org/10.1109/ACCESS.2020.3011456.

[32] N. Jankovic, J. Roldan-Perez, M. Prodanovic, L. Rouco, Centralised Multimode Power Oscillation Damping Controller for Photovoltaic Plants with Communication Delay Compensation, 13 de abril de 2023, *arXiv*: arXiv:2304.06415. Accedido: 15 de diciembre de 2023. [En línea]. Disponible en: http://arxiv.org/abs/2304.06415.

[33] Basu M, Mahindara VR, Kim J, Nelms RM, Muljadi E. Comparison of Active and Reactive Power Oscillation Damping With PV Plants. IEEE Trans. on Ind. Applicat. 2021;57(3):2178–86. https://doi.org/10.1109/TIA.2021.3059810.

[34] Jankovic N, Roldan-Perez J, Prodanovic M, Suul JA, D'Arco S, Rodriguez LR. Power oscillation damping method suitable for network reconfigurations based on converter interfaced generation and combined use of active and reactive powers. Int. J. Electr. Power Energy Syst. 2023;149. https://doi.org/10.1016/j.ijepes.2023.109010.

[35] A. Arvani, V.S. Rao, Power oscillation damping controller for the power system with high wind power penetration level, en *2014 North American Power Symposium (NAPS)*, Pullman, WA, USA: IEEE, sep. 2014, pp. 1-6. doi: 10.1109/NAPS.2014.6965400.

[36] S. Alalwani, S. Isik, S. Bhattacharya, Inter-area Oscillation Damping Controller for DFIG based Wind Power Plants, en *2022 IEEE Energy Conversion Congress and Exposition (ECCE)*, Detroit, MI, USA: IEEE, oct. 2022, pp. 1-6. doi: 10.1109/ECCE50734.2022.9947750.

[37] L. Petersen, P.H. Nielsen, G.C. Tarnowski, T. Lund, Addressing power oscillations damping requirements for wind power plants, en *20th International Workshop on Large-Scale Integration of Wind Power into Power Systems as well as on Transmission Networks for Offshore Wind Power Plants (WIW 2021)*, Hybrid Conference, Germany: Institution of Engineering and Technology, 2021, pp. 403-413. doi: 10.1049/icp.2021.2642.

[38] Leon AE, Solsona JA. Power oscillation damping improvement by adding multiple wind farms to wide-area coordinating controls. IEEE Trans. Power Syst. 2014;29 (3):1356–64. https://doi.org/10.1109/TPWRS.2013.2289970.

[39] Domínguez-García JL, Gomis-Bellmunt O, Bianchi FD, Sumper A. Power oscillation damping supported by wind power: A review. Renew. Sustain. Energy Rev. 2012; 16(7):4994–5006. https://doi.org/10.1016/j.rser.2012.03.063.

[40] Surinkaew T, Ngamroo I. Coordinated Robust Control of DFIG Wind Turbine and PSS for Stabilization of Power Oscillations Considering System Uncertainties. IEEE Trans. Sustain. Energy 2014;5:823–33. https://doi.org/10.1109/TSTE.2014.2308358.

[41] D.S. Restrepo, M.A. Rios, «Adaptive POD for STATCOM in a Power System with High Wind Power Penetration Level», en *2019 IEEE Workshop on Power Electronics and Power Quality Applications (PEPQA)*, Manizales, Colombia: IEEE, may 2019, pp. 1-6. doi: 10.1109/PEPQA.2019.8851562.

[42] Edrah M, et al. «Effects of POD Control on a DFIG Wind Turbine Structural System», jun. IEEE Trans. Energy Convers. 2020;vol. 35, n.o 2:765–74. https://doi.org/10.1109/TEC.2020.2966181.

[43] Yang S, et al. Optimal node selection of damping controller for power systems with high wind power penetration. Int. J. Electr. Power Energy Syst. 2022;136:107716. https://doi.org/10.1016/j.ijepes.2021.107716.

[44] He P, Wen F, Ledwich G, Xue Y. An investigation on interarea mode oscillations of interconnected power systems with integrated wind farms. Int. J. Electr. Power Energy Syst. 2016;78:148–57. https://doi.org/10.1016/j.ijepes.2015.11.052.

[45] «PowerFactory DIgSILENT». [En línea]. Disponible en: https://www.digsilent.de/en/powerfactory.html.

[46] DIgSILENT PowerFactory, «IEEE 39 Bus New Engalnd system».

[47] M.A. Pai, *Energy Function Analysis for Power System Stability*. Boston, MA: Springer US, 1989. doi: 10.1007/978-1-4613-1635-0.

[48] «Website of the IEEE PES PSDPC SCS, Task Force on Benchmark Systems for Stability Controls: "39 bus system Base Case" and PDF-document "39bus.out" (39bus.pdf), http://www.sel.eesc.usp.br/ieee/IEEE39/ base.htm (downloaded in May 2014)».

[49] MINISTERIO DE INDUSTRIA, TURISMOY COMERCIO, «Procedimiento de Operación 13.1. "Criterios de Desarrollo de la Red de Transporte",» mar. 2005.